ACS OMEGA

Open Access



http://pubs.acs.org/journal/acsodf

Article

# Transparent X-ray Shielding Solutions with Various Metal Ions

Ryoma Tokonami, Minoru Osanai, Masahiro Hosoda, Shinji Tokonami, and Tatsuhiro Takahashi*

Cite This: *ACS Omega* 2024, 9, 44770−44777

Read Online

ACCESS | Metrics & More | Article Recommendations

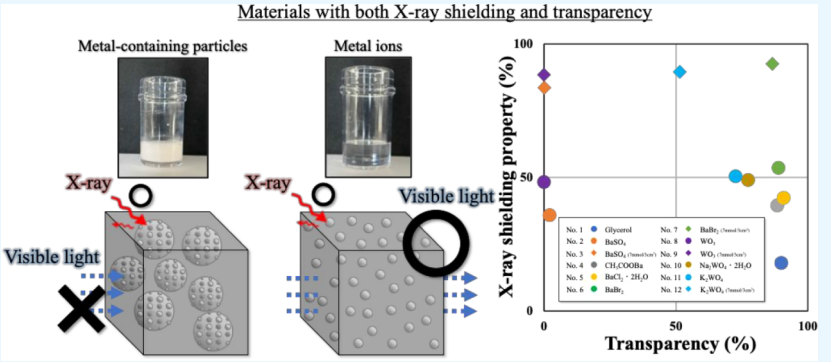


**ABSTRACT:** We fabricated transparent, Pb-free X-ray shielding materials using solvated ions in a polar solvent. Previous materials have been based on dispersions of metal-containing particles such as barium sulfate ($BaSO_4$) in a matrix. Comparisons of suspensions of metal-based particles and solutions of metal ions in a solvent enable better understanding of interactions such as reflection, scattering, and absorption between X-rays and substances. The X-ray shielding properties of a solution of solvated metal ions were similar to or better than those of suspensions of metal-containing particles. In addition, the metal-ion solutions exhibited high transparency. The most effective material among those investigated for X-ray shielding was barium bromide ($BaBr_2$), which exhibits high solubility in polar solvents. X-ray shielding of 92% was confirmed at a tube voltage of 120 kV, along with ∼90% UV transmittance at a visible-light wavelength of 400 nm. Thus, both high X-ray shielding performance and high transparency were achieved.

## 1. INTRODUCTION

Radiation such as gamma-rays and X-rays is composed of electromagnetic waves with high energy. Such radiation is used in various fields, including the medical, nuclear power, and aerospace industries. Radiation shielding materials play an important role in protecting people who work in these fields against radiation exposure. Pb, in particular, has been widely used for radiation shielding because of its low cost, high atomic number, and ease of processing; however, it has significant drawbacks, including high toxicity and a high mass density. To develop Pb-free radiation shielding materials, researchers have investigated composites containing metal particles such as barium sulfate ($BaSO_4$) and tungsten(VI) oxide ($WO_3$) mixed with resin or rubber.[1−5] These composites were evaluated from the perspectives of mechanical properties and radiation shielding performance. Research involving metal particles for radiation shielding tends to focus on particle size, types of particles, the quantities of particles incorporated into a matrix, and the interface between the matrix and filler materials. Composites composed of acrylonitrile−butadiene−styrene (ABS) and microscale metal particles of compounds such as $WO_3$ and bismuth oxide ($Bi_2O_3$) combine a high metal particle content with flexibility.[6] Research on radiation shielding materials based on a matrix of biodegradable resins such as starch and poly(vinyl alcohol) (PVA), rather than resin or rubber, has also been reported.[7] Composites composed of wood and $Bi_2O_3$ as a filler have been studied to improve both mechanical properties and X-ray shielding.[8] X-ray shielding garments with air and water vapor permeability have been investigated as new radiation shielding materials.[9] Nanoparticles have been found to provide more effective radiation shielding than microparticles because of enhanced interaction between the radiation and the metal particles.[10−13] A leather X-ray shielding material consisting of Bi and I has been developed to achieve balance between X-ray shielding properties and water-vapor permeability.[14] Also, X-ray shielding materials based on nanofibers and nanometal particles have attracted attention because of their unusual

Received: August 28, 2024
Revised: October 10, 2024
Accepted: October 22, 2024
Published: October 28, 2024

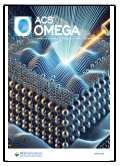

properties, which include high flexibility.[15,16] In recent research, we found that surface modification using multiwalled carbon nanotubes (MWCNTs) can improve interfacial adhesion between the matrix and fillers without affecting the X-ray shielding properties.[17] The X-ray shielding properties are strongly correlated with atomic number, favoring the use of metals such as Bi, W, and Ba. In recent years, technologies for radiation shielding materials with not only good radiation shielding performance but also good flexibility, high biodegradability, low toxicity, and low mass density have advanced dramatically; thus, the development of radiation shielding materials with additional beneficial properties is important in this field.

Pb-based glass has been one of the most effective materials for achieving a balance between X-ray shielding performance and transparency.[18,19] However, Pb-based glass is heavy, toxic, and difficult to process. As alternatives, Pb-free transparent radiation shielding materials have been developed by dispersing nanometal particles.[20,21] Metal particles have been investigated not only in radiation shielding materials but also in composites with high transparency, where metal particles with a size smaller than visible wavelengths ($400 \leq \lambda \leq 800$ nm) were polymerized.[22−24] Even if metal particles can be polymerized to a diameter of 20 nm, their transparency is reduced because of their agglomeration by van der Waals forces.[25] Thus, these methods are not suitable for radiation shielding materials that require a large amount of metal. Barium carbonate ($BaCO_3$) was dispersed in PVA to prepare an X-ray shielding material; however, $BaCO_3$ can only be added in very small quantities because it increases particle agglomeration.[26] In cases where metal particles are used, achieving both high X-ray shielding performance and high transparency is difficult. An alternative approach is radical copolymerization using two Bi-based monomers.[27] However, the resultant composites exhibit a yellow appearance characteristic of Bi and their fabrication process is complex. The use of Bi is incompatible with complete transparency. Thus, achieving both transparency and good radiation shielding performance is difficult using conventional technologies.

In the present study, Ba- and W-containing compounds that can be dissolved in a polar solvent such as water or glycerol were investigated. The resultant solutions were evaluated for both X-ray shielding performance and transparency, and the results were compared with those for metal particles reported in previous studies. Comparisons of metal ions and metal particles were conducted to understand interactions such as reflection, scattering, and absorption between X-rays and target materials. Solutions were prepared with the same number of heavy-metal Ba and W atoms per unit volume in polar solvents, and the interaction between X-rays and the metals was evaluated. This comparison was important in this study because metal particles have a crystalline structure that is also expected to reflect and scatter X-rays. Such a comparison of metal-containing particles and solvated metal ions has not been previously reported. The X-ray shielding properties were evaluated using diagnostic X-ray high-voltage equipment, and transparency was evaluated using UV−visible spectrophotometry. In addition, the results obtained experimentally were compared with simulation results obtained using the web-based software XCOM. Various soluble compounds were investigated to determine which solutions provide the greatest X-ray shielding capacity and transparency. The results led to novel approaches as alternatives to metal-containing particles such as $Bi_2O_3$ and $BaSO_4$ as X-ray shielding materials.

## 2. EXPERIMENTS

**2.1. Materials.** Glycerol (Kanto Chemical) with a density of 1.26 g/cm$^3$ was used as a polar solvent because of its high boiling point and high viscosity. $BaSO_4$ (Takehara Kagaku Kogyo) with a particle diameter of 10 $\mu$m and a density of 4.50 g/cm$^3$ and tungsten(VI) oxide ($WO_3$; Tokyo Chemical) with a particle diameter of 30 $\mu$m and a density of 7.16 g/cm$^3$ were used as poorly soluble metal-containing compounds. Barium acetate ($CH_3COOBa$; Fujifilm Wako Pure Chemical) with a density of 2.47 g/cm$^3$, barium chloride dihydrate ($BaCl_2\cdot 2H_2O$; Fujifilm Wako Pure Chemical) with a density of 3.10 g/cm$^3$, barium bromide ($BaBr_2$; Tokyo Chemical) with a density of 4.78 g/cm$^3$, sodium tungstate dihydrate ($Na_2WO_4\cdot 2H_2O$; Fujifilm Wako Pure Chemical) with a density of 4.18 g/cm$^3$, and potassium tungstate ($K_2WO_4$; Fujifilm Wako Pure Chemical) with a density of 3.12 g/cm$^3$ were used as glycerol-soluble metal compounds. All of the chemicals and their suppliers are given in Table 1.

**2.2. Preparation of Solutions of Dissolved Metal Ions.** Table 2 shows the solution density, weight percent against total, and appearance of all 12 prepared samples. All of the samples were prepared with the same volume of 3 cm$^3$. The solution density was calculated from the amount of solution consisting of glycerol and each metal compound and from the total volume of 3 cm$^3$. Samples with metal particles and metal ions were prepared such that the samples contained the same number of metal atoms such as barium atoms and tungsten atoms, enabling us to confirm that even samples containing dissolved metal ions exhibit X-ray shielding properties. All of the solutions were placed in polystyrene containers for evaluation of their X-ray shielding properties. Samples were prepared such that the number of metal atoms in the total volume was 1 mmol/3 cm$^3$ or 7 mmol/3 cm$^3$. Thus, the number of metal atoms present per unit volume was compared for two different types of samples: solids dispersed in glycerol and solutions of metal salts dissolved in glycerol. All samples other than those containing $BaSO_4$ or $WO_3$ were dissolved in glycerol under heating at 80 °C using a hot plate for 1 day because they did not dissolve in glycerol at room temperature. $CH_3COOBa$, $BaCl_2\cdot 2H_2O$, and $Na_2WO_4\cdot 2H_2O$ could not be dissolved to a concentration of 7 mmol/3 cm$^3$. The respective weight percentages are also reported in Table 2. The maximum solubility of the samples did not change after a number of runs; in addition, the dissolved samples were left at room temperature for more than 1 month without recrystallizing, confirming that they continued to dissolve.

**2.3. Preparation of Samples for X-ray Shielding Experiments.** The setup used for the X-ray shielding measurements is shown in Figure 1. The distance between the X-ray source and detector was 100 cm, and a 0.45 cm Pb plate was placed on the detector to minimize the effect of scattered X-rays. The Pb plate had a 1.5 cm hole through its center. A diagnostic X-ray high-voltage apparatus (Shimadzu, UD150L-40F) was used. The X-ray shielding properties were evaluated under a tube voltage of 40−120 kV, tube current 200 mA, and irradiation time of 200 ms. The X-ray transmittance was calculated as $I/I_0$, where $I_0$ is the intensity of incident X-rays and $I$ is the intensity of transmitted X-rays. Some formulas were used to evaluate the X-ray shielding properties from


https://doi.org/10.1021/acsomega.4c07904
ACS Omega 2024, 9, 44770−44777

Table 1. All Chemicals Used in This Work

| Material | Glycerol | Barium sulfate ($BsSO_4$) | Tungsten(III) oxide ($WO_3$) | Barium acetate ($CH_3COOBa$) | Barium chloride dihydrate ($BaCl_2{\cdot}2H_2O$) | Barium bromide ($BaBr_2$) | Sodium tungstate(IV) dihydrate ($Na_2WO_4{\cdot}2H_2O$) | Potassium tungstate ($K_2WO_4$) |
|---|---|---|---|---|---|---|---|---|
| Density ($g/cm^3$) | 1.26 | 4.50 | 7.16 | 2.47 | 3.10 | 4.78 | 4.18 | 3.12 |
| Purity (%) | 99.5 | 98.0 | 99.9 | 99.9 | 98.0 | 98.0 | 99.0 | 97.0 |
| Molar mass (g/mol) | 92.1 | 233.38 | 3.29.85 | 214.45 | 244.26 | 297.14 | 329.85 | 326.03 |
| Supplier | Kanto Chemical Co., Ltd. | Takehara kagaku Kogyo Co., Ltd. | Tukyo Chemical Co., Inc. | Fujifilm Wako Pure Chemical Corp. | Fujifilm Wako Pure Chemical Corp. | Tokyo Chemical Co., Inc. | Fujifilm Wako Pure Chemical Corp. | Fujifilm Wako Pure Chemical Carp. |
| Information | | Particle size 10 $\mu m$ | Particle size 30 $\mu m$ | | | | | |

various perspectives. X-ray shielding properties were evaluated according to eqs 1−3:

$$I = I_0\, e^{-\mu x} \tag{1}$$

$$\mu = \mu_m \times \rho \tag{2}$$

$$\mathrm{HVL} = \frac{\ln(2)}{\mu} \tag{3}$$

where $x$, $\rho$, $\mu$, $\mu_m$, and HVL are the thickness of the solution, its density, the linear attenuation coefficient, the weight attenuation coefficient, and the half-value layer, respectively. The solution thickness, $x$, was 0.66 cm. A detector (Unfors RaySafe, RaySafe X2) was used to measure the X-ray intensity. Each sample was irradiated five times. Samples No. 2, No. 3, No. 8, and No. 9 were irradiated after being thoroughly stirred to prevent precipitation of $BaSO_4$ and $WO_3$. X-ray shielding properties determined by experiment were compared with the calculation results obtained in simulations using the XCOM software (National Institute of Standards and Technology, USA). For the XCOM simulations, the weight attenuation coefficient for the energy was automatically calculated using the adjusted proportion of glycerol and metal particles or metal compounds as a parameter. The values calculated by XCOM simulations were compared with experimental data reported in a previous study.[28]

**2.4. Preparation of Solutions for Transparency Measurements.** The transparency of solutions was evaluated using a UV−visible spectrophotometer (U-4100, Hitachi High-Tech). The range of measured wavelengths was 400−800 nm, covering most of the visible wavelength range. Also, the dimensions of the cell used for the measurements were 12.5 mm × 12.5 mm × 45 mm. Dispersions containing metal particles such as $BaSO_4$ or $WO_3$ were measured after the dispersions were thoroughly stirred. Measurements of transparent solutions were conducted three times; representative data are shown in the results.

## 3. RESULTS AND DISCUSSION

**3.1. Determination of Solubility in Each Solution.** We investigated the solubility of each of the other chemicals. $CH_3COOBa$, $BaCl_2{\cdot}2H_2O$, and $Na_2WO_4{\cdot}2H_2O$ exhibited low solubility and $BaBr_2$ and $K_2WO_4$ exhibited high solubility in glycerol. Samples No. 7 ($BaBr_2$, 38.34 wt %) and No. 12 ($K_2WO_4$, 42.81 wt %) were prepared as saturated solutions. The $Na_2WO_4{\cdot}2H_2O$ and $K_2WO_4$ solutions were light-yellow (Table 2).

**3.2. X-ray Shielding Properties.** Figure 2a−p shows the X-ray shielding properties of the prepared solutions. In each figure, samples dispersed in glycerol as metal particles are indicated as (P) and those dissolved as metal ions are indicated as (I). Specifically, Figure 2a−d shows the X-ray transmittance, Figure 2e−h shows the linear attenuation coefficient, and Figure 2i−l shows the mass attenuation coefficient. The results in Figure 2a indicate that the concentration of Ba atoms is 1 mmol/3 $cm^3$. Glycerol alone is not expected to exhibit a substantial X-ray shielding effect. We compared samples No. 2 and No. 3 to demonstrate the difference in X-ray shielding effect between metal-containing particles and metal ions and to clarify the interaction between X-rays and metals. The X-ray shielding effect of $BaSO_4$ has been reported in various studies.[28,29] The results show that the X-ray transmittance of glycerol decreased upon the addition of $BaSO_4$ (No. 2). In the



https://doi.org/10.1021/acsomega.4c07904
ACS Omega 2024, 9, 44770−44777

**Table 2. Suspensions of $BaSO_4$ and $WO_3$ and Solutions of $BaCl_2{\cdot}2H_2O$, $BaBr_2$, $Na_2WO_4{\cdot}2H_2O$, and $K_2WO_4$ in Glycerol, as Prepared for X-ray Shielding Measurements**

| Atom | - | Ba | | | | | | W | | | | |
|---|---|---|---|---|---|---|---|---|---|---|---|---|
| Chemical | Glycerol | $BaSO_4$ | | $CH_3COOBa$ | $BaCl_2 \cdot 2H_2O$ | $BaBr_2$ | | $WO_3$ | | $Na_2WO_4 \cdot 2H_2O$ | $K_2WO_4$ | |
| No. | 1 | 2 | 3 | 4 | 5 | 6 | 7 | 8 | 9 | 10 | 11 | 12 |
| Total volume | 3 $cm^3$ | 3 $cm^3$ | 3 $cm^3$ | 3 $cm^3$ | 3 $cm^3$ | 3 $cm^3$ | 3 $cm^3$ | 3 $cm^3$ | 3 $cm^3$ | 3 $cm^3$ | 3 $cm^3$ | 3 $cm^3$ |
| Number of mol in total volume | 0 mmol / 3 $cm^3$ | 1 mmol / 3 $cm^3$ | 7 mmol / 3 $cm^3$ | 1 mmol / 3 $cm^3$ | 1 mmol / 3 $cm^3$ | 1 mmol / 3 $cm^3$ | 7 mmol / 3 $cm^3$ | 1 mmol / 3 $cm^3$ | 7 mmol / 3 $cm^3$ | 1 mmol / 3 $cm^3$ | 1 mmol / 3 $cm^3$ | 7 mmol / 3 $cm^3$ |
| Solution density | 1.26 $g/cm^3$ | 1.32 $g/cm^3$ | 1.68 $g/cm^3$ | 1.31 $g/cm^3$ | 1.32 $g/cm^3$ | 1.34 $g/cm^3$ | 1.81 $g/cm^3$ | 1.33 $g/cm^3$ | 1.73 $g/cm^3$ | 1.34 $g/cm^3$ | 1.33 $g/cm^3$ | 1.78 $g/cm^3$ |
| Weight percent against total | 0 wt% | 5.89 wt% | 32.35 wt% | 6.49 wt% | 6.19 wt% | 7.40 wt% | 38.34 wt% | 5.83 wt% | 31.35 wt% | 8.18 wt% | 8.15 wt% | 42.81 wt% |
| Appearance |  | | | | | | | | | | | |

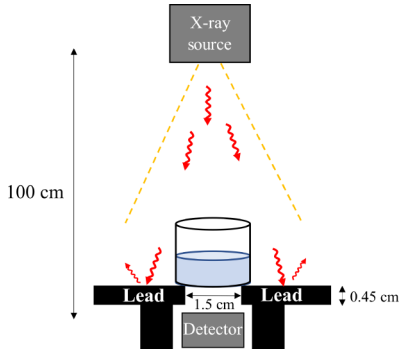


**Figure 1.** Setup for X-ray shielding measurements using a solution.

case of sample No. 3 containing a suspension of $BaSO_4$ particles, a slight decrease in X-ray transmittance was confirmed, which is attributed not to reflection and scattering but to absorption resulting from the interaction between X-rays and the metal ions. Thus, irrespective of the structure of the metal-containing compounds, they can shield against X-rays when existing as free metal ions. The literature contains no reports comparing the X-ray shielding properties of metal-containing particles and metal ions solvated in a polar solvent. In addition, the X-ray transmittance of sample No. 4 ($CH_3COOBa$) was slightly lower than that of No. 3 ($BaSO_4$). The results further demonstrate that $Cl^-$ as a counterion in $BaCl_2{\cdot}2H_2O$ enhanced the X-ray shielding effect. Moreover, the X-ray transmittance of sample No. 6 ($BaBr_2$) was substantially lower than those of the $BaSO_4$ suspension and the $CH_3COOBa$ and $BaCl_2{\cdot}2H_2O$ solutions. These results suggest that, among the samples investigated in the present study, 1 mmol/3 $cm^3$ $BaSO_4$ (No. 2) might not be suitable as an X-ray shielding material.

Figure 2b shows the results for the samples with a W atom content of 1 mmol/3 $cm^3$. No distinct differences were observed between samples No. 10 and No. 11; however, the X-ray transmittance for samples No. 10 and No. 11 containing solvated W ions dissolved in glycerol was slightly lower than that of sample No. 8 containing $WO_3$ particles. Figure 2c,d shows the case of 7 mmol/3 $cm^3$, where the X-ray transmittance for both samples No. 7 and No. 12 was less than 0.1. Figure 2e−h confirms that several of the solutions are effective X-ray shielding materials.

Figure 2i−l, which was prepared by calculation from the results in Figure 2e−h, plays an important role in verifying the correctness and reliability of the experimental results. Table 3 shows two types of mass attenuation coefficients obtained by experiment and by simulation using XCOM under conditions of 60 kV as the tube voltage (average energy 30 keV). Different values were obtained between the experimental and simulation results for both sample No. 9 and No. 12, which contained high concentrations of W atoms. However, the differences between the experimental and simulation results for these samples is attributable to the experimental X-ray energy having a wide range and the X-ray energy in the XCOM simulations having a discrete energy. In addition, in a previous study, a lower energy was reported to correspond to a greater difference in each mass attenuation coefficient obtained from XCOM simulations.[30] Furthermore, the HVL values also indicate that the X-ray shielding properties of metal particles and metal ions in glycerol were approximately the same (Figure 2m−p).

Numerous approaches have been proposed for improving the radiation shielding properties of materials, such as using metals with high atomic numbers and achieving a good dispersion of metal particles.[11,12,31,32] The X-ray shielding effect can be improved through the use of nanoparticles. Numerous researchers have focused on Bi because it exhibits greater X-ray activity than Ba and W.[3,10,14,27,28,31] However, a large amount of metal per unit volume can be achieved by dissolving metals as ions. In addition, the X-ray shielding properties of solutions containing metal ions can be further improved through the selection of appropriate counter ions. In the case of $BaBr_2$, not only $Ba^{2+}$ ions but also $Br^-$ ions demonstrated X-ray shielding properties. Improving X-ray shielding properties by dissolving ions in a polar solvent and using X-ray-shielding counterions in addition to heavy-metal atoms has not been previously reported.

**3.3. Transparency.** The results of transparency measurements are presented in Figure 3a−d. Figure 3a,b corresponds to Ba atoms at concentrations of 1 mmol/3 $cm^3$ and 7 mmol/3


https://doi.org/10.1021/acsomega.4c07904
ACS Omega 2024, 9, 44770−44777

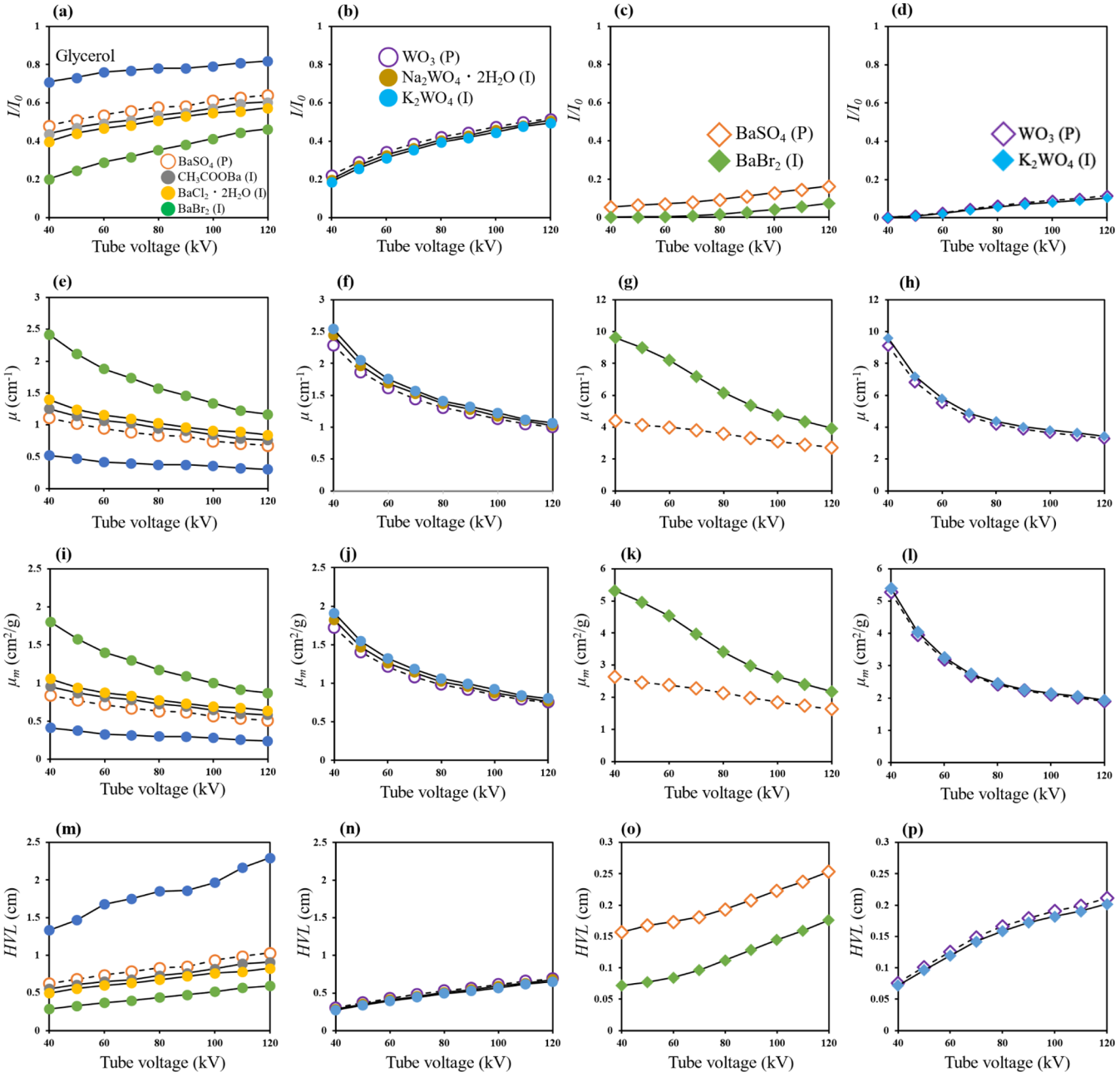


**Figure 2.** X-ray shielding properties, including X-ray transmittance ($I/I_0$), linear attenuation coefficient ($\mu$), mass attenuation coefficient ($\mu_m$), and half-value layer (HVL) of all of the investigated samples: (a) $I/I_0$ for Ba at 1 mmol/3 $cm^3$; (b) $I/I_0$ for W at 1 mmol/3 $cm^3$; (c) $I/I_0$ for Ba at 7 mmol/3 $cm^3$; (d) $I/I_0$ for W at 7 mmol/3 $cm^3$; (e) $\mu$ for Ba at 1 mmol/3 $cm^3$; (f) $\mu$ for W at 1 mmol/3 $cm^3$; (g) $\mu$ for Ba at 7 mmol/3 $cm^3$; (h) $\mu$ for W at 7 mmol/3 $cm^3$; (i) $\mu_m$ for Ba at 1 mmol/3 $cm^3$; (j) $\mu_m$ for W at 1 mmol/3 $cm^3$; (k) $\mu_m$ for Ba at 7 mmol/3 $cm^3$; (l) $\mu_m$ for W at 7 mmol/3 $cm^3$; (m) HVL for Ba at 1 mmol/3 $cm^3$; (n) HVL for W at 1 mmol/3 $cm^3$; (o) HVL for Ba at 7 mmol/3 $cm^3$; and (p) HVL for W at 7 mmol/3 $cm^3$.

**Table 3. Experimental and Simulated Mass Attenuation Coefficients for Prepared Solutions Containing Various Metal Atoms (60 kV Tube Voltage)**

| | No.1 | No.2 | No.3 | No.4 | No.5 | No.6 | No.7 | No.8 | No.9 | No.10 | No.11 | No.12 |
|---|---|---|---|---|---|---|---|---|---|---|---|---|
| $\mu_m$ ($cm^2$/g) from experiment | 0.33 | 0.71 | 2.38 | 0.81 | 0.87 | 1.40 | 4.54 | 1.22 | 3. 19 | 1.26 | 1.32 | 3.26 |
| $\mu_m$ ($cm^2$/g) from simulation | 0.33 | 0.68 | 2.24 | 0.76 | 0.76 | 1.34 | 5.57 | 1.37 | 5.9 | 1.48 | 1.42 | 6.06 |

$cm^3$, respectively, and Figure 3b,d corresponds to W atoms at concentrations of 1 mmol/3 $cm^3$ and 7 mmol/3 $cm^3$, respectively. Solutions consisting of $Ba^{2+}$ ions at a concentration of 1 mmol/3 $cm^3$ were confirmed to exhibit a UV transmittance ratio of ∼90% from the results in Figure 3a. In particular, all of the samples exhibited high visible-light transmittance at wavelengths from 400 to 800 nm, consistent with their clear and colorless appearance. High transparency is also evident in Figure 3b; however, the UV transmittance was lower—less than 70−80%—in the wavelength range 400−600



https://doi.org/10.1021/acsomega.4c07904
ACS Omega 2024, 9, 44770−44777

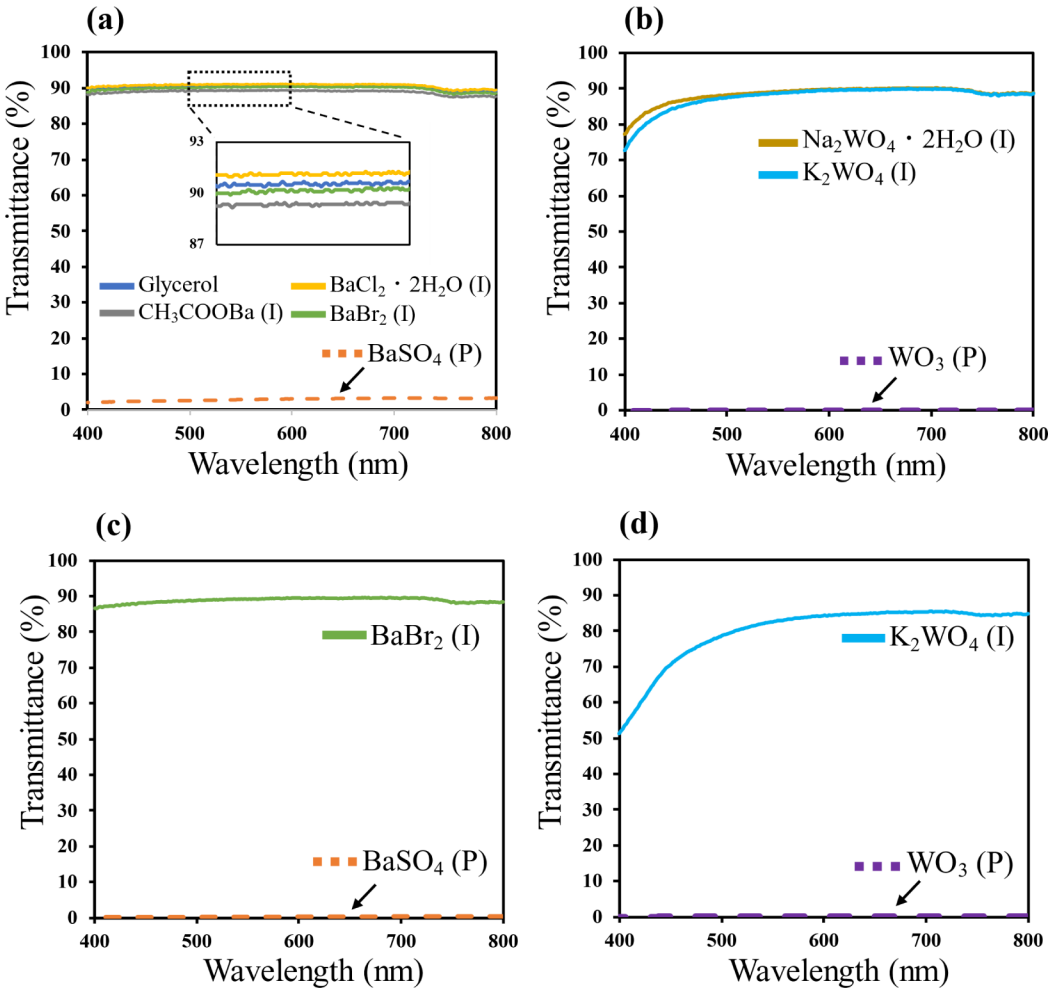


**Figure 3.** Visible-light transmittance for (a) Ba at 1 mmol/3 $cm^3$, (b) W at 1 mmol/3 $cm^3$, (c) Ba at 7 mmol/3 $cm^3$, and (d) W at 7 mmol/3 $cm^3$.

nm. This observation is attributed to the slight yellow coloration resulting from the dissolution of $Na_2WO_4{\cdot}2H_2O$ and $K_2WO_4$. The solution with $WO_3$ dispersed in glycerol showed almost no transmission and was totally opaque. Figure 3c shows the results for Ba at a concentration of 7 mmol in 3 $cm^3$ of glycerol. $BaBr_2$ (No. 7) exhibited high transparency even when dissolved at a high concentration. The visible-light transmittance for $K_2WO_4$ at 7 mmol/3 $cm^3$ (No. 12) was slightly lower than that for only glycerol (No. 1) (Figure 3d). In addition, the transmittance for sample No. 12 at 400 nm was 50% (Figure 3d), which can be explained by the high concentration of dissolved W causing the solution to turn yellow. By contrast, the visible-light transmittance for solutions of dispersed $BaSO_4$ and $WO_3$ was less than 1.0%. Thus, suspensions prepared using metal-containing particles such as $BaSO_4$ and $WO_3$ cannot be transparent.

**3.4. Correlation between X-ray Shielding Properties and Transparency and Determination of Optimal Metal Compounds.** Both the X-ray shielding properties and transparency of the 12 prepared samples are shown in Figure 4, where X-ray shielding is plotted on the vertical axis and transparency on the horizontal axis. The conditions corresponding to the vertical and horizontal axes are a tube voltage of 120 kV and a visible-light wavelength of 400 nm. The X-ray shielding percentage was calculated by subtracting the transmittance, $I/I_0$, from 1. Here, $I/I_0$ indicates the X-ray

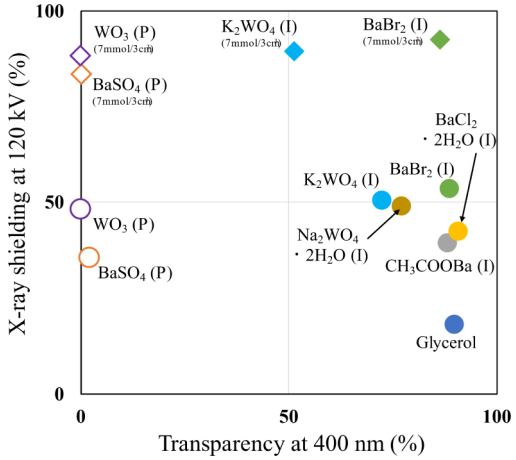


**Figure 4.** Scatter plot of solutions prepared using glycerol, $BaSO_4$, $CH_3COOBa$, $BaCl_2{\cdot}2H_2O$, $BaBr_2$, $WO_3$, $K_2WO_4{\cdot}2H_2O$, and $K_2WO_4$, evaluated under a tube voltage of 120 kV and transparency at 400 nm to determine the most effective compound for X-ray shielding.

transmittance, whereas the X-ray shielding indicates the material's ability to protect against X-rays. When the intensities of the incident and transmitted X-rays are equal, in the absence of a sample, a value of 1 was calculated in the X-ray transmission measurement. The sample whose data point is plotted in the top-right corner in Figure 4 can be considered to



https://doi.org/10.1021/acsomega.4c07904
ACS Omega 2024, 9, 44770−44777

exhibit both good X-ray shielding properties and high transparency. The literature contains few reports demonstrating X-ray shielding evaluations under a high tube voltage of 120 kV. For this reason, the X-ray shielding properties corresponding to a low tube voltage for composites containing a metal can be drastically decreased by the effect of various interactions with low-energy X-rays.[17] In addition, for transparent composites, the visible-light transmittance at 400 nm tends to be lower than that at 800 nm.[33] In the case of dispersions of metal-containing particles such as $BaSO_4$ and $Bi_2O_3$ in glycerol, visible light could not be transmitted under any of the investigated conditions (Figure 3). However, samples consisting of dissolved metal ions exhibited X-ray transmittance that was approximately the same as or better than that observed for the metal-containing particle dispersions, and their high visible transmittance was confirmed. In the case of $K_2WO_4$, the results show that it exhibits both unsatisfactory X-ray shielding and unsatisfactory transparency. However, compared with solutions that contain metal particles, solutions of solvated $K_2WO_4$ exhibit greater transparency but with coloration. In this research, the solution that demonstrated the best combination of X-ray shielding performance and transparency was $BaBr_2$ (No. 7). Its X-ray shielding ratio and transparency ratio were 92.6% and 86.5%, respectively. $K_2WO_4$ (No. 12) exhibited a high X-ray shielding ratio but its visible-light transmittance was only ∼50%. The UV transmittance of silica glasses with high transparency has been reported to be ∼60% at 400 nm.[34] Thus, the combination of high X-ray shielding and complete transparency have not been achieved in any previous study.

## 4. CONCLUSION

X-ray shielding materials that exhibit both complete transparency and high X-ray shielding performance were investigated, and the role of the interactions between the metal and X-rays was evaluated by comparison of suspensions of metal-containing particles and solutions of metal ions. $BaBr_2$ and $K_2WO_4$ exhibited high solubility of 38.34 and 42.81 wt %, respectively, in glycerol. As a result, solutions of dissolved metal ions demonstrated better X-ray shielding performance than suspensions of metal-containing particles such as $BaSO_4$ and $WO_3$ in samples prepared such that the number of metal atoms was the same. The results indicate that the interaction between X-rays and metal ions was absorption, not scattering or reflection. In addition, the visible-light transmittance for solutions dissolved as metal ions in glycerol differed substantially from that for samples of suspended metal-containing particles. We decided that the most effective material for both high X-ray shielding and high transparency is $BaBr_2$, which exhibited an X-ray shielding ratio of 92.6% at a thickness of 0.66 cm even at a higher tube voltage of 120 kV, and visible-light transmission of 86.5% even at the shorter visible-light wavelength of 400 nm. We thus concluded that $BaBr_2$ dissolved in glycerol is an X-ray shielding material with both high X-ray shielding performance and high transparency. Completely transparent X-ray shielding materials will be useful, especially in the medical field, as an alternative to Pb-glass. In addition, dissolving metal ions in a polar solvent is expected to be an important approach in applications that require transparent X-ray shielding materials.

## AUTHOR INFORMATION


### Corresponding Author

**Tatsuhiro Takahashi** − *Graduate School of Organic Materials Science, Yamagata University, Yonezawa, Yamagata 992-8510, Japan*; Email: effort@yz.yamagata-u.ac.jp

### Authors

**Ryoma Tokonami** − *Graduate School of Organic Materials Science, Yamagata University, Yonezawa, Yamagata 992-8510, Japan*; orcid.org/0009-0009-0349-5065

**Minoru Osanai** − *Hirosaki University Graduate School of Health Sciences, Hirosaki, Aomori 036-8564, Japan*

**Masahiro Hosoda** − *Hirosaki University Graduate School of Health Sciences, Hirosaki, Aomori 036-8564, Japan; Institute of Radiation Emergency Medicine, Hirosaki University, Hirosaki, Aomori 036-8564, Japan*

**Shinji Tokonami** − *Institute of Radiation Emergency Medicine, Hirosaki University, Hirosaki, Aomori 036-8564, Japan*

Complete contact information is available at: https://pubs.acs.org/10.1021/acsomega.4c07904


### Author Contributions

R.T. and T.T. conceived and designed the project. R.T., O.M., M.H., and S.T. conducted the X-ray shielding measurements. All of the authors discussed the results and commented on the manuscript.

### Notes

The authors declare no competing financial interest.

## ACKNOWLEDGMENTS

This work was supported by JKA through its promotion funds from KEIRIN RACE Grant number 2024M-490 and JSPS Grant-in-Aid for JSPS Fellows Grant number 24KJ0449.

## REFERENCES


(1) Poltabtim, W.; Wimolmala, E.; Saenboonruang, K. Properties of lead-free gamma-ray shielding materials from metal oxide/EPDM rubber composites. *Radiat. Phys. Chem.* **2018**, *153*, 1−9.

(2) Li, Q.; Wang, Y.; Xiao, X.; Zhong, R.; Liao, J.; Guo, J.; Liao, X.; Shi, B. Research on X-ray shielding performance of wearable Bi/Ce-natural leather composite materials. *J. Hazard. Mater.* **2020**, *398*, 122943.

(3) Cheraghi, E.; Chen, S.; Liu, J. A.; Sun, Y.; Yeow, J. T. W. Lightweight and flexible bismuth oxide composite with enhanced x-ray shielding efficiency. *J. Appl. Polym. Sci.* **2022**, *139* (45), No. e53130.

(4) Mesbahi, A.; Ghiasi, H. Shielding properties of the ordinary concrete loaded with micro- and nano-particles against neutron and gamma radiations. *Appl. Radiat. Isot.* **2018**, *136*, 27−31.

(5) Tiamduangtawan, P.; Wimolmala, E.; Meesat, R.; Saenboonruang, K. Effects of Sm2O3 and Gd2O3 in poly (vinyl alcohol) hydrogels for potential use as self-healing thermal neutron shielding materials. *Radiat. Phys. Chem.* **2020**, *172*, 108818.

(6) Olivieri, F.; Avolio, R.; Gentile, G.; Mazzone, A.; Rizzi, R.; Nacucchi, M.; Castaldo, R.; Errico, M. E.; Giannini, C.; Ambrosio, L.; et al. High filler content acrylonitrile-butadiene-styrene composites containing tungsten and bismuth oxides for effective lead-free x-ray radiation shielding. *Polym. Compos.* **2024**, *45*, 2101.

(7) Atta, M. M.; Abou-Laila, M. T.; Abdelwahed, M. H.; Dwidar, S. A.; Desouky, O. Structural, mechanical, and thermal features of PVA/starch/graphene oxide nanocomposite enriched with WO3 as gamma−ray radiation shielding materials for medical applications. *Polym. Sci. Eng.* **2023**, *63* (11), 3843−3854.

(8) Poltabtim, W.; Wimolmala, E.; Markpin, T.; Sombatsompop, N.; Rosarpitak, V.; Saenboonruang, K. X-ray Shielding, Mechanical, Physical, and Water Absorption Properties of Wood/PVC Composites Containing Bismuth Oxide. *Polymers* **2021**, *13* (13), 2212.
(9) Quan, J.; Wang, H.; Li, T.; Fan, L.; Yu, J.; Wang, Y.; Zhu, J.; Hu, Z. Air and Water Vapor Permeable UHMWPE Composite Membranes for X-Ray Shielding. *Ind. Eng. Chem. Res.* **2020**, *59* (19), 9136−9142.
(10) Tiamduangtawan, P.; Kamkaew, C.; Kuntonwatchara, S.; Wimolmala, E.; Saenboonruang, K. Comparative mechanical, self-healing, and gamma attenuation properties of PVA hydrogels containing either nano- or micro-sized Bi2O3 for use as gamma-shielding materials. *Radiat. Phys. Chem.* **2020**, *177*, 109164.
(11) Asari Shik, N.; Gholamzadeh, L. X-ray shielding performance of the EPVC composites with micro- or nanoparticles of WO3, PbO or Bi2O3. *Appl. Radiat. Isot.* **2018**, *139*, 61−65.
(12) Kim, S.-C. Analysis of Shielding Performance of Radiation-Shielding Materials According to Particle Size and Clustering Effects. *Appl. Sci.* **2021**, *11* (9), 4010.
(13) Nambiar, S.; Osei, E. K.; Yeow, J. T. W. Polymer nanocomposite-based shielding against diagnostic X-rays. *J. Appl. Polym. Sci.* **2013**, *127* (6), 4939−4946.
(14) Wang, Y.; Ding, P.; Xu, H.; Li, Q.; Guo, J.; Liao, X.; Shi, B. Advanced X-ray Shielding Materials Enabled by the Coordination of Well-Dispersed High Atomic Number Elements in Natural Leather. *ACS Appl. Mater. Interfaces* **2020**, *12* (17), 19916−19926.
(15) Sobczak, J.; Truszkiewicz, A.; Korczeniewski, E.; Cyganiuk, A.; Terzyk, A. P.; Kolanowska, A.; Jedrysiak, R. G.; Boncel, S.; Zyla, G. Shape-Controlled Iron-Paraffin Composites as gamma- and X-ray Shielding Materials Formable by Warmth-of-Hands-Derived Plasticity. *ACS Appl. Eng. Mater.* **2023**, *1* (12), 3237−3253.
(16) Xu, L.; Huang, L.; Yu, J.; Si, Y.; Ding, B. Ultralight and Superelastic Gd(2)O(3)/Bi(2)O(3) Nanofibrous Aerogels with Nacre-Mimetic Brick-Mortar Structure for Superior X-ray Shielding. *Nano Lett.* **2022**, *22* (21), 8711−8718.
(17) Tokonami, R.; Osanai, M.; Hosoda, M.; Tokonami, S.; Takahashi, T. Simple surface modification of barium sulfate for improving the interface of polymer composites and its x-ray shielding properties. *Polym. Compos.* **2024**, *45*, 7519−7529.
(18) Noor Azman, N. Z.; Siddiqui, S. A.; Ionescu, M.; Low, I. M. A comparative study of X-ray shielding capability in ion-implanted acrylic and glass. *Radiat. Phys. Chem.* **2013**, *85*, 102−106.
(19) Mukamil, S.; Ullah, I.; Sarumaha, C.; Wabaidur, S. M.; Islam, M. A.; Khattak, S. A.; Kothan, S.; Shoaib, M.; Khan, I.; Ullah, I.; et al. Lead-borate glass system doped with Sm3+ ions for the X-ray shielding applications. *Results Phys.* **2022**, *43*, 106121.
(20) Khazaalah, T. H.; Mustafa, I. S.; Sayyed, M. I.; Abdul Rahman, A.; Mohd Zaid, M. H.; Hisam, R.; Izwan Abdul Malik, M. F.; Seth Ezra, N.; Salah Naeem, H.; Che Khalib, N. Development of Novel Transparent Radiation Shielding Glasses by BaO Doping in Waste Soda Lime Silica (SLS) Glass. *Sustainability* **2022**, *14* (2), 937.
(21) Kaewjaeng, S.; Kothan, S.; Chaiphaksa, W.; Chanthima, N.; Rajaramakrishna, R.; Kim, H. J.; Kaewkhao, J. High transparency La2O3-CaO-B2O3-SiO2 glass for diagnosis x-rays shielding material application. *Radiat. Phys. Chem.* **2019**, *160*, 41−47.
(22) Nam, H.; Seo, D.; Yun, H.; Thangavel, G.; Park, L.; Nam, S. Transparent Conducting Film Fabricated by Metal Mesh Method with Ag and Cu@Ag Mixture Nanoparticle Pastes. *Metals* **2017**, *7* (5), 176.
(23) Wang, W.; Zhang, B.; Jiang, S.; Bai, H.; Zhang, S. Use of CeO(2) Nanoparticles to Enhance UV-Shielding of Transparent Regenerated Cellulose Films. *Polymers* **2019**, *11* (3), 458.
(24) Han, X.-W.; Zeng, X.-F.; Zhang, J.; Huan, H.; Wang, J.-X.; Foster, N. R.; Chen, J.-F. Synthesis of transparent dispersion of monodispersed silver nanoparticles with excellent conductive performance using high-gravity technology. *J. Chem. Eng.* **2016**, *296*, 182−190.
(25) Sumida, K.; Hiramatsu, K.; Sakamoto, W.; Yogo, T. Synthesis of transparent BaTiO3 nanoparticle/polymer hybrid. *J. Nanopart. Res.* **2007**, *9* (2), 225−232.
(26) Muhammad, N. A.; Armynah, B.; Tahir, D. High transparent wood composite for effective X-ray shielding applications. *Mater. Res. Bull.* **2022**, *154*, 111930.
(27) Matsumura, Y.; Horikoshi, H.; Furukawa, K.; Miyamoto, M.; Nishimura, Y.; Ochiai, B. Synthesis of Bismuth-Containing Polymer Films with High Refractive Index and X-ray Shielding Property by Radical Polymerization of Styrylbismuthine Derivatives. *ACS Macro Lett.* **2022**, *11* (6), 723−726.
(28) Thumwong, A.; Chinnawet, M.; Intarasena, P.; Rattanapongs, C.; Tokonami, S.; Ishikawa, T.; Saenboonruang, K. A Comparative Study on X-ray Shielding and Mechanical Properties of Natural Rubber Latex Nanocomposites Containing Bi2O3 or BaSO4: Experimental and Numerical Determination. *Polymers* **2022**, *14* (17), 3654.
(29) Lopresti, M.; Palin, L.; Alberto, G.; Cantamessa, S.; Milanesio, M. Epoxy resins composites for X-ray shielding materials additivated by coated barium sulfate with improved dispersibility. *Mater. Today Commun.* **2021**, *26*, 101888.
(30) Daneshvar, H.; Milan, K. G.; Sadr, A.; Sedighy, S. H.; Malekie, S.; Mosayebi, A. Multilayer radiation shield for satellite electronic components protection. *Sci. Rep.* **2021**, *11* (1), 20657.
(31) Intom, S.; Kalkornsurapranee, E.; Johns, J.; Kaewjaeng, S.; Kothan, S.; Hongtong, W.; Chaiphaksa, W.; Kaewkhao, J. Mechanical and radiation shielding properties of flexible material based on natural rubber/ Bi2O3 composites. *Radiat. Phys. Chem.* **2020**, *172*, 108772.
(32) Toyen, D.; Wimolmala, E.; Sombatsompop, N.; Markpin, T.; Saenboonruang, K. Sm2O3/UHMWPE composites for radiation shielding applications: Mechanical and dielectric properties under gamma irradiation and thermal neutron shielding. *Radiat. Phys. Chem.* **2019**, *164*, 108366.
(33) Magrini, T.; Bouville, F.; Lauria, A.; Le Ferrand, H.; Niebel, T. P.; Studart, A. R. Transparent and tough bulk composites inspired by nacre. *Nat. Commun.* **2019**, *10* (1), 2794.
(34) Kotz, F.; Quick, A. S.; Risch, P.; Martin, T.; Hoose, T.; Thiel, M.; Helmer, D.; Rapp, B. E. Two-Photon Polymerization of Nanocomposites for the Fabrication of Transparent Fused Silica Glass Microstructures. *Adv. Mater.* **2021**, *33* (9), No. e2006341.


https://doi.org/10.1021/acsomega.4c07904
*ACS Omega* 2024, 9, 44770−44777